Experimental Neurology 167, 215–226 (2001)
doi:10.1006/exnr.2000.7551, available online at http://www.idealibrary.com on IDEAL®

ST14A Cells Have Properties of a Medium-Size Spiny Neuron

Michelle E. Ehrlich,*[,1] Luciano Conti,†[,1] Mauro Toselli,‡ Luca Taglietti,‡ Edgardo Fiorillo,‡ Vanni Taglietti,‡ Sanja Ivkovic,* Barbara Guinea,* Anna Tranberg,* Simonetta Sipione,† Dorotea Rigamonti,† and Elena Cattaneo†

*The Nathan S. Kline Institute for Psychiatric Research, Orangeburg, New York 10962-2210; †Institute of Pharmacological Sciences, University of Milano, Via Balzaretti 9, 20133 Milan, Italy; and ‡Dipartimento di Fisiologia e Farmacologia Cellulare e Molecolare, INFM Pavia Unit, Pavia, Italy

Received January 7, 2000; accepted August 22, 2000; published online December 14, 2000

The ST14A cell line was previously derived from embryonic day 14 rat striatal primordia by retroviral transduction of the temperature-sensitive SV40 large T antigen. We showed that cell division and expression of nestin persists at 33°C, the permissive temperature, whereas cell division ceases, nestin expression decreases, and MAP2 expression increases at the nonpermissive temperature of 39°C. In this study, we further characterized the cells and found that they express other general and subtype-specific neuronal characteristics. ST14A cells express enolase and βIII-tubulin. Furthermore, they express the striatal marker DARPP-32, which is up-regulated upon differentiation of the cells by growth in serum-free medium. Stimulation with dopamine, the D2-dopamine receptor agonist quinpirole, or the D1-dopamine receptor agonist SKF82958 results in phosphorylation of CREB. Treatment of the cells with a mixture of reagents which stimulate the MAPK and adenylyl cyclase pathways radically changes the morphology of the ST14A cells. The cells develop numerous neurite-like appearing processes which stain with βIII-tubulin. Moreover, under these conditions, intracellular injection of rectangular depolarizing current stimuli elicits overshooting action potentials with a relatively fast depolarization rate when starting from a strongly hyperpolarized membrane potential. Taken together, these data imply that the ST14A cell line displays some of the characteristics of a medium-size spiny neuron subtype and provides a new tool to elucidate the pathways and molecules involved in medium-size spiny neuron differentiation and disease.

INTRODUCTION

The medium-size spiny neuron (MSN) comprises 95% of the neurons of the caudate putamen, or the rodent striatum. This neuronal subtype plays a major role in sensorimotor and cognitive functions and in many neuropsychiatric diseases. MSNs use γ-aminobutyric acid (GABA) as their primary neurotransmitter and are morphologically homogeneous. The MSNs, however, are biochemically heterogeneous, with subpopulations expressing various combinations of receptors, neuropeptides, and signal transduction molecules (reviewed in 16). Therefore, primary neuronal cultures derived from striatal progenitor cells are also extremely heterogeneous, making the study of the biology of subtypes of MSNs technically difficult. Moreover, many studies cannot be performed on the small amount of tissue provided by primary cultures. Immortalized neuronal cell lines represent a tool for the study of the biology of specific neuronal subtypes, but few cell lines representative of differentiated neurons have been established. Several techniques have been utilized, including the use of spontaneously transformed cells, e.g., PC12 (17), oncogene-containing retroviral vectors (1, 13, 14, 22, 30, 31, 34–36, 41–43), and somatic cell fusion (40). Cell lines already in existence have contributed significantly to the study of neurons in general and to specific features of the medium-size spiny neuron (40).

We have previously described the growth characteristics of the ST14A cell line, derived from embryonic day 14 (E14) rat striatal primordia by retroviral transduction of the temperature-sensitive ts A58/U19 allele of SV40 large T antigen (6). Unlike cells derived from somatic fusion (40), cell lines derived in this manner contain a normal complement of chromosomes without contamination from a neuroblastoma cell line. They have a built-in method to maintain or cease mitosis and therefore potentially represent an alternative model for the generation of an unlimited supply of material for the study of the medium-size spiny neuron. The ST14A cell line was previously chosen from among many clones for more extensive analysis because it exhibited a high proliferative ability at 33°C

[1] Co-first author.

0014-4886/00 $35.00

(6). Cell division and expression of nestin persists at 33°C, the permissive temperature, whereas cell division ceases, nestin expression decreases, and MAP2 expression increases at the nonpermissive temperature of 39°C. Expression of the glial marker, glial fibrillary acidic protein, was not detected. Differentiation of the ST14A cells was also demonstrated following intracerebral grafting procedures (24). Under these conditions, ST14A cells were shown to develop into postmitotic, differentiated neurons and glia, suggesting that the immortalized cells truly represent a bipotential CNS progenitor. More detailed studies performed by other investigators showed that similarly derived cells transplanted into the developing CNS undergo a differentiation pathway that morphologically and antigenically resembles that of the surrounding host cells (31, 35). However, information on the *in vitro* properties of the immortalized cells is required since it contributes to defining the potential and limits of such cells. In this study, we sought to determine whether ST14A cells demonstrate other phenotypic and electrophysiologic characteristics of neurons and, particularly, whether they are representative of a medium-size spiny neuron.

EXPERIMENTAL PROCEDURES

ST14A Cell Line

The establishment of the ST14A cell line was previously described in detail (6). Cells are propagated at the permissive temperature of 33°C in Dulbecco's modified Eagle medium (Life Technologies, Bethesda, MD) supplemented with 0.11 g/liter sodium pyruvate, 3.7 g/liter sodium bicarbonate, 0.29 g/liter glutamine, 3.9 g/liter Hepes, 100 units/ml penicillin–streptomycin (Life Technologies), plus 10% fetal calf serum. Division ceases at the nonpermissive temperature in identical medium which includes serum or at the permissive temperature in the absence of serum. Pharmacologic treatments included acidic fibroblast growth factor (aFGF; 10 ng/ml), phorbol 12-myristate 13-acetate (TPA; 200 nM), dopamine (10–50 μM), isobutylmethylxanthine (IBMX; 0.25 mM), forskolin (50 μM), SKF82958 (50 μM), quinpirole (10–60 μM), and eticlopride (40 μM). All reagents were from Sigma except SKF82958, quinpirole, and eticlopride (RBI).

Immunocytochemistry

Cultures were grown on LabTek eight-well slides coated with laminin and fixed in 4% paraformaldehyde in 0.1 M phosphate buffer (pH 7.4). Cultures were then processed with the appropriate primary and secondary antibodies using the immunoperoxidase/ABC method (Vector Laboratories Elite Vectastain) or with a FITC-conjugated antibody (Sigma). Antibodies used were neuron-specific enolase (1:1000; Polyscience, Inc.), GABA (1:1000; Sigma), βIII-tubulin (1:200; Promega), actin (1:1000; Sigma), DARPP-32 6a (1:20,000; from Dr. Paul Greengard, The Rockefeller University, New York, NY), ARPP-21 6a (1:10,000; from Dr. Paul Greengard, The Rockefeller University), and phospho-CREB (1:1000; Upstate Biotechnology).

Determination of Adenylyl Cyclase Activity

Adenylyl cyclase activity was measured as described in Unterwald *et al.* (39). Crude membranes were prepared from ST14A cells from individual cultures, and 10 μl of homogenate was incubated in 10 mM imidazole (pH 7.4), 10 mM theophylline, 6 mM $MgSO_4$, 0.6 mM EGTA, 1.5 mM ATP, and 0.01 mM GTP, in the absence or presence of 10 μM dopamine or forskolin (final reaction volume 60 μl). The reaction was terminated by boiling for 2 min, and the amount of cAMP formed was determined utilizing a [^{3}H]cAMP binding protein assay which is based on the separation of free cAMP from that bound to the binding protein.

Western Blot Analysis

Proteins were derived from rapidly frozen cultures grown in 35- or 60-mm dishes, which were not coated. Total cellular protein was prepared according to the manufacturer's instructions (TRIzol; Gibco BRL) or via lysis in boiling sample buffer (20% glycerol, 62.5 mM Tris–HCl, pH 6.9, 1% SDS, 5% β-mercaptoethanol, 0.025% bromophenol blue) followed by sonication, 15 min of centrifugation, and recovery of the supernatants. Western blot analysis with 20–40 μg of protein was performed on 10% SDS–polyacrylamide gels. Following transfer to nitrocellulose, equal loading of proteins was confirmed by Ponceau stain. Western blot analysis was performed as previously described (8, 20) and developed with the NEN–DuPont chemiluminescence system.

Solutions for Electrophysiological Recording

Seals between electrodes and cells were established in a bath solution consisting of (in mmol/liter): 135 NaCl, 1.8 $CaCl_2$, 2 $MgCl_2$, 5.5 KCl, 10 glucose, 10 Hepes/NaOH (pH 7.4). After establishing the whole-cell configuration, for current-clamp recording and for K^+ current recording in voltage clamp, the pipette filling solution contained (in mmol/liter): 140 KCl, 4 NaCl, 0.02 $CaCl_2$, 0.8 EGTA, 2 $MgCl_2$, 4 Mg-ATP, 10 Hepes/KOH (pH 7.4). For the study of voltage-gated Na^+ and Ca^{2+} channels under voltage-clamp conditions, the patch pipette was filled with (in mmol/liter): 130 CsCl, 10 NaCl, 20 TEA-Cl, 10 EGTA, 2 $MgCl_2$, 4 Mg-ATP, 10 Hepes/CsOH (pH 7.4). To dissect Na^+ currents the extracellular solution contained (in mmol/liter): 130 NaCl, 2 $CaCl_2$, 2 $MgSO_4$, 10 glucose, 5 tetraethylam-

monium-Cl, 10 Hepes/NaOH (pH 7.4). For voltage-gated Ca^{2+} channel current recordings, extracellular saline contained (in mmol/liter): 130 NaCl, 10 $BaCl_2$, 2 $MgCl_2$, 10 glucose, 10 Hepes/NaOH (pH 7.4), 1 4-aminopyridine, 10 tetraethylammonium-Cl, 1.5×10^{-3} tetrodotoxin. For K^+ channel current recordings, extracellular saline contained (in mmol/liter): 13 NaCl, 4 KCl, 2 $CaCl_2$, 1.2 $MgSO_4$, 220 glucose, 10 Hepes/KOH (pH 7.4), 1 CdCl, 1.5×10^{-3} tetrodotoxin. A multibarrel delivery system positioned close to the cell allowed a fast exchange of external solutions, useful for a pharmacological characterization of the different conductances.

Patch-Clamp Recording

Ionic currents were recorded under voltage-clamp conditions using the patch-clamp whole-cell configuration (19) at room temperature (20–24°C) with a LIST LM/EPC7 patch-clamp amplifier (List Electoronic, Darmstadt, Germany) and digitized at sampling intervals of 26–100 μs using a 12-bit A/D Tecmar Lab Master Board interfaced with an IBM-compatible PC. Stimulation, acquisition, and data analysis were carried out using the following software packages: pClamp (Axon Instruments, Inc., Burlingame, CA) and Origin (Microcal Software, Inc., Northampton, MA). For voltage-clamp experiments linear components of leak and capacitive currents were first reduced by analogue circuitry and then almost completely canceled with the P/N method. Patch pipettes were made from borosilicate glass tubing and fire polished. For current-camp experiments, their tips were coated with Sylgard to reduce capacitance. Pipettes had a final resistance of 1–2 MΩ when filled with internal solution. Currents were filtered at 3 kHz.

RESULTS

Undifferentiated ST14A Cells Express General and Subtype-Specific Neuronal Markers

It was previously shown that ST14A cells express low levels of MAP2 in the undifferentiated state and that expression of this neuronal-specific marker is first down-regulated and then markedly up-regulated during growth in serum-free medium (SFM) for up to 168 h (6). ST14A cells also express neuron-specific enolase (NSE) (Fig. 1a) and βIII-tubulin (Fig. 4) when grown in fetal calf serum. These data imply that even in the immortalized, mitotic state, the ST14A cells are expressing antigens typically characteristic of neurons which have progressed beyond the progenitor state. When differentiated by growth in SFM or at the nonpermissive temperature, all ST14A cells continue to express NSE (not shown). This contrasts with *in vivo* data demonstrating that ST14A cells give rise to both neurons and glia after transplantation (24), implying that extracellular cues encountered after transplantation can induce ST14A differentiation toward a glial lineage.

We next sought to determine whether the undifferentiated ST14A cells also express more subtype-specific neuronal markers, specifically those associated with the striatal medium-size spiny neuron. We found that ST14A cells are immunopositive for GABA (Fig. 1b). However, almost 100% of primary neurons derived from the E14 lateral ganglionic eminence are immunopositive for GABA and/or glutamic acid decarboxylase (GAD_{67}) after only 1 day *in vitro* (21). These data suggest that the presence of this neurotransmitter-synthesizing enzyme, and even the neurotransmitter itself, is not an index of a terminally differentiated phenotype. We therefore examined the ST14A cell line for expression of DARPP-32, a dopamine- and cyclic AMP-regulated phosphoprotein expressed in 98% of the medium-size spiny neurons (28). This marker was found by immunocytochemistry (not shown) and was also easily detected by Western blot analysis (Fig. 2A). The protein or mRNA for ARPP-21, another dopamine- and cyclic AMP-regulated phosphoprotein expressed in the majority of MSNs but structurally unrelated to DARPP-32 (27), was undetectable, even following RT-PCR (not shown).

To demonstrate that the expression of DARPP-32 was not an artifact of the immortalization procedure, we examined similarly generated lines from the striatum (ST86 and ST79-13a; Cattaneo, unpublished) and from the hippocampus (HiB5) (31). We found that high levels of DARPP-32 were specific to the ST14A cell line (Fig. 2A).

Differentiated ST14A Cells Up-regulate Neuronal Markers

As described above, ST14A cells are induced to differentiate by growth at the nonpermissive temperature of 39°C in the presence of serum and/or growth in serum-free media at either the permissive or the nonpermissive temperature. We previously reported that the combination of removal of serum with a shift in temperature up to 39°C causes ST14A cell death within 2–3 days of incubation (6, 32). Therefore, most of the studies of the phenotype of the ST14A cells were originally performed at 33°C in the presence or absence of serum, and we continued with this protocol in the current study. Under either differentiating condition, the cells ceased dividing, down-regulated nestin expression, and up-regulated MAP2 expression. The morphology of the cells, however, did not radically change. They continued to grow in a monolayer, retained a flat morphology, and were somewhat ameboid in appearance. There was no appearance of being connected by processes, which remained very stunted (6) (Fig. 1b).

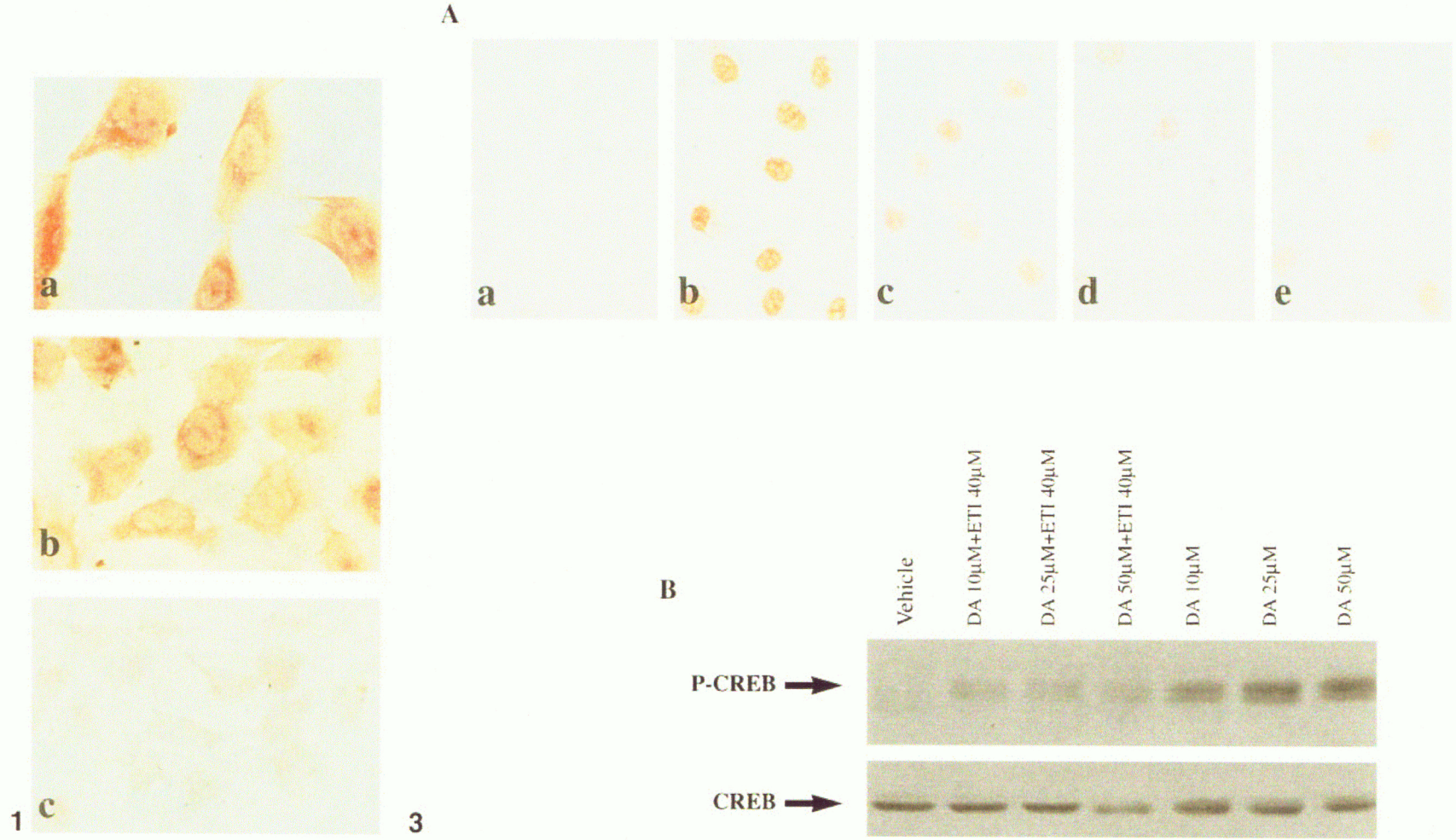

FIG. 1. ST14A cells express neuronal-specific markers. ST14A cells are immunocytochemically positive for neuronal-specific enolase (a) when grown at the permissive temperature, 33°C, in fetal calf serum. (b) Like medium-size spiny neurons, ST14A cells are also immunopositive for GABA. The staining is specific as revealed by omission of the primary antibody in a sister culture (c).

FIG. 3. Induction of phosphorylation of CREB by treatment of ST14A cells with dopamine or a D1-dopamine receptor agonist. (A) Immunocytochemistry for phospho-CREB in (a) ST14A cells treated with vehicle, (b) cells exposed to 10 μM forskolin for 15 min, (c) cells exposed to dopamine (50 μM) for 15 min, (d) cells exposed to SKF82958 (50 μM) for 15 min, and (e) cells exposed to quinpirole (60 μM) for 10 min. (B) Western blot analysis for phospho-CREB. ST14A cells were grown in SFM at 33°C for 48 h and then exposed to vehicle or dopamine (10, 25, 50 μM) alone or in the presence of eticlopride (40 μM) for 15 min. Cells were then harvested in boiling lysis buffer, and 25 μg of protein from each sample was subjected to SDS–PAGE, followed by Western analysis with an antibody specific for phospho-Ser133-CREB. Vehicle-treated cells were negative at 5 min, and dopamine and forskolin-treated cells were already positive, but with lower levels of P-CREB detectable at that time point (not shown).

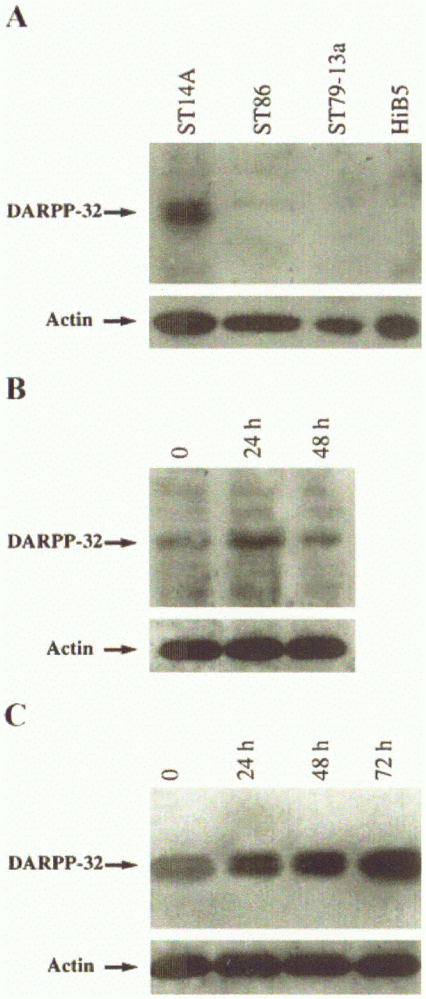

FIG. 2. ST14A cells express DARPP-32. (A) Western analysis of DARPP-32 in 20 μg of cell extract from ST14A, ST86, ST79-13a, and HiB5 cells. All ST lines were derived from the rat striatal primordia, whereas the HiB5 cell line was derived from the hippocampal primordium (31). Western analysis of the same blot with an anti-actin antibody demonstrates equal amounts of protein in all four lanes. (B) Levels of DARPP-32 protein increase over the first 24 h of growth at the nonpermissive temperature, 39°C, in the absence of serum, but are already decreasing by 48 h, likely due to cell death. (C) Levels of DARPP-32 protein increase steadily over a much longer period of growth at 33°C, also in the absence of serum.

We therefore looked for molecular evidence of differentiation. We found that the amount of DARPP-32 protein increases after growth for 24 h in SFM at 39°C, but then begins to decrease, possibly due to impending cell death (Fig. 2B). In SFM at 33°C, DARPP-32 levels increase gradually for 3–5 days (Fig. 2C), consistent with the previously described increase in MAP-2 levels.

ST14A Cells Have Functional Dopamine Receptors

Medium-size spiny neurons receive major dopaminergic input from the midbrain. All MSNs are dopaminoceptive, expressing one, or more than one, of the dopamine receptor subtypes (37). To determine whether ST14A cells express functional dopamine receptors, we examined the phosphorylation of the cyclic AMP response-element binding protein (CREB) (7, 44) by immunocytochemistry or Western analysis following stimulation with either dopamine, the D1-receptor agonist SKF82958, or the D2-receptor agonist quinpirole. In a nonquantitative demonstration, P-CREB was detected in the nucleus following stimulation with all three agents (Fig. 3A). Phosphorylation of CREB following stimulation with dopamine was confirmed by Western analysis and was dose-dependent (Fig. 3B). Eighty percent of the phosphorylation of CREB by dopamine, 10 or 25 μM, was eliminated by pretreatment with the D2-receptor antagonist, eticlopride (Fig. 3B), whereas phosphorylation of CREB was not reproducibly diminished by pretreatment with the D1-receptor agonist, SCH23390 (data not shown). These data dem-

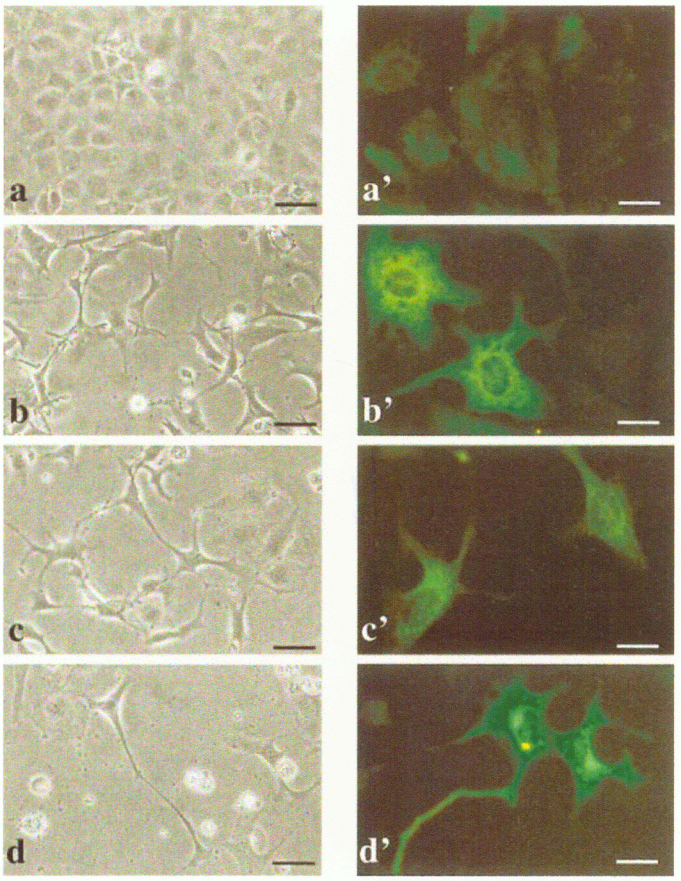

FIG. 4. Induction of morphologic neuronal differentiation in ST14A cells grown in "differentiation mix." Cells were grown in acidic fibroblast growth factor (10 ng/ml), phorbol 12-myristate 13-acetate (200 nM), dopamine (20 μM), isobutylmethylxanthine (0.25 mM), and forskolin (50 μM) and then immunocytochemically stained for βIII-tubulin. (a–d) Microphotographs of the culture at the different time points; scale bar, 25 μm. (a′–d′) Immunocytochemical assay of the culture at different time points performed with anti βIII-tubulin antibody; scale bar, 10 μm. (a–a′) Baseline, (b–b′) 24 h, (c–c′) 48 h, (d–d′) 72 h.

onstrated the presence of both D2-like and D1-like receptors, but implied that the majority of the receptors which contributed to the phosphorylation of CREB were of the D2-like subtype. D1-subtype receptors are positively linked to adenylyl cyclase, so we measured baseline and dopamine-stimulated adenylyl cyclase activity. Forskolin, which directly stimulates the adenylyl cyclase and bypasses the membrane receptor, stimulated adenylyl cyclase activity greater than fivefold ($N = 4$), but dopamine-stimulated cyclase activity was either the same as basal ($N = 2$) or slightly increased above basal levels (10% above control; $N = 2$). This is similar to what is seen in the prenatal and newborn rodent striatum, but is also consistent with the majority of the ST14A dopamine receptors being of the D2-like subtype (33).

Morphologic and Physiologic Differentiation of ST14A Cells by "Dopamine Differentiation Mix"

Many immortalized neuronal cell lines of various origin are known to differentiate in the presence of agents which lead to an increase in intracellular cAMP levels, e.g., forskolin and butyrate (e.g., 17, 29). In an attempt to further differentiate the ST14A cells, we treated them with a mixture of reagents which stimulate the MAPK, adenylyl cyclase, and protein kinase C pathways. This mix, labeled the "dopamine differentiation mix," was previously described in experiments which led to transdifferentiation from a GABAergic to a dopaminergic phenotype in cultured striatal neurons (10). This mixture consists of aFGF (10 ng/ml), TPA (200 nM), dopamine (20 μM), IBMX (0.25 mM), and forskolin (50 μM). When this mixture was applied to ST14A cells for 4 days at 33°C, in the presence or absence of serum, the morphology of the cells radically changed. Division markedly slowed, even in the presence of serum. As usual, the cells remained in a monolayer. Most important, the cells developed numerous neurite-like appearing processes which grew progressively over the 3 days observed (Figs. 4a–4d). These processes stained with βIII-tubulin, and the staining intensity for this marker appeared to increase over the same time period (Figs. 4a′–4d′). Of note, there was marked variability between neurons, so that not all developed the identical morphology, especially in terms of length of neurites (Figs. 4d and 4d′).

To examine whether the morphologically differentiated ST14A cells had electrical characteristics of neurons, we performed electrophysiologic determinations. In a series of 24 *in vitro* differentiated ST14A cells perfused with intra- and extracellular salines that roughly simulate physiological intra- and extracellular fluids, the resting potential had a mean value of -31 ± 11 mV. Under current-clamp conditions, intracellular injection of rectangular depolarizing current stimuli from the resting potential could hardly elicit regenerative voltage responses in these cells, even with very large current stimuli (>150 pA). This difficulty in generating action potentials could be overcome in a fraction of ST14A cells by starting from a hyperpolarizing membrane potential as shown in Fig. 5A. In this case, voltage responses that became regenerative for current stimuli >75 pA could be obtained. In the same cell, after switching to whole-cell voltage-clamp mode, a pattern of currents was elicitable by membrane depolarization in which voltage-gated inward and outward currents coexisted, with features, at first sight, similar to the Na and K channel currents responsible for action potential in neurons (Fig. 5B).

Isolation and Time Course of a Voltage-Gated Na Current in ST14A Cells

Figure 5C shows a family of inward current recordings obtained during whole-cell voltage-clamp steps to various membrane potentials in an *in vitro* differentiated ST14A cell using bath and pipette filling solutions suitable for the isolation of Na currents. This current turned on at about −40 mV and its peak amplitude increased up to 0 mV. Activation sped up with increasing membrane depolarization. Inactivation was fast and complete. Superfusion of ST14A cells with 1.5 μM tetrodotoxin (TTX) caused a reversible current reduction of about 30% ($N = 4$), as shown in the inset of Fig. 5C (upper tracings). Furthermore the inward current was strongly reduced by decreasing extracellular [Na^+] from 130 to 13 mM, as shown in the inset of Fig. 5C (lower tracings). These observations clearly demonstrate that the inward current, observed in about 70% of the clamped ST14A cells ($N = 34$), is a voltage-gated Na current with low sensitivity to the Na channel blocker TTX.

The peak I–V relationship for an eight-cell sample obtained over a voltage range between −40 and +70 mV and starting from a holding potential of −70 mV is shown in Fig. 5D. It reached a peak at 0 mV and the extrapolated reversal potential was about +80 mV.

The activation characteristics of the Na current were analyzed by estimating the conductance (g) at different depolarizations according to the relation $I_{Na} = g\,(V - E_{Na})$, where I_{Na} refers to peak current values. The data were then fitted to the Boltzmann equation $g = g_{max}/\{1 + \exp[(V - V_{½})/k]\}$. The maximum conductance, g_{max}, was 6.1 ± 3.9 nS ($N = 8$). The average normalized conductance is shown in Fig. 5E, in which the half-activation potential, $V_{½}$, and the slope, k, were −21.9 and −7.7 mV, respectively. The voltage dependence of Na current inactivation (h_∞) was studied by measuring the peak Na current elicited at −10 mV following a conditioning potential of variable amplitude and 600 ms duration to allow the inactivation variable to reach

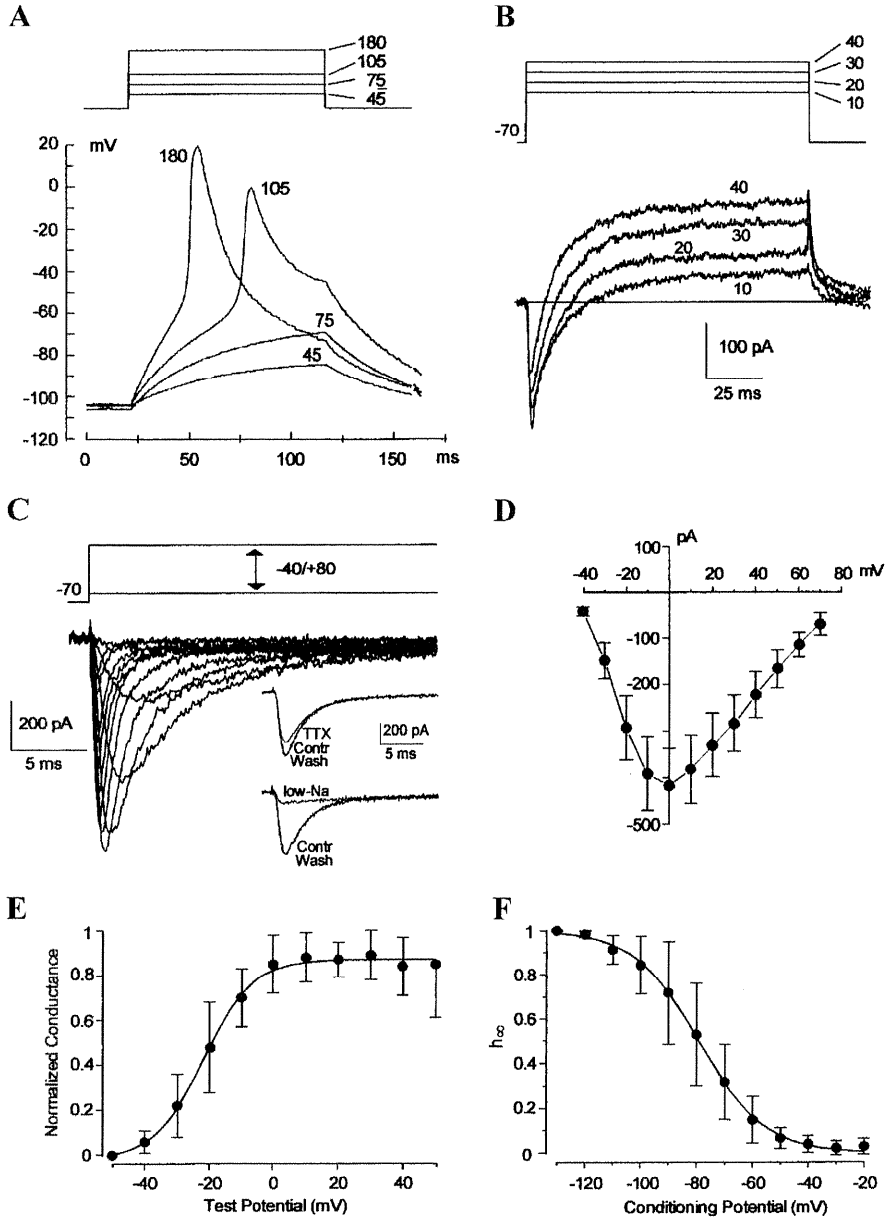

FIG. 5. Voltage and current responses of *in vitro* differentiated ST14A cells. (A) Superimposed voltage responses were obtained under current-clamp conditions using 140 mM K^+ intracellularly. The cell was stimulated with rectangular current pulses of increasing amplitude (protocol shown over the voltage tracings). (B) Superimposed inward and outward current tracings obtained at the indicated membrane potentials immediately after voltage recordings shown in (A) by switching from current to voltage clamp. The voltage pulse protocol is illustrated over the current tracings. (C) Voltage-dependent activation of full inactivating outward currents in a ST14A cell. Superimposed current traces were elicited in control intra- and extracellular saline appropriate to isolate Na current (see Experimental Procedures), using the voltage pulse protocols illustrated over the current tracings. (Inset) Upper tracings: outward currents were recorded at −10 mV from the same cell as in (C), before (Contr), during application of 1.5 μM TTX (TTX), and during wash out (Wash). Lower tracings: outward currents were recorded at −10 mV from the same cell as in (C), in control saline (Contr), during application of an extracellular saline containing a 10-fold lower Na^+ concentration (low-Na), and during wash out (Wash). (D) Average of the peak Na current amplitude vs voltage (N = 8); bars denote standard errors; holding potential −70 mV. (E) Average normalized conductance–voltage relation. Data are represented as means and SD (N = 8); the continuous line through data points is the least-squares best fit of the Boltzmann equation $g_{norm} = 1/\{1 + \exp[(V - V_{½})/k]\}$, where $V_{½}$ and k are −21.9 and −7.7 mV, respectively. (F) Average steady-state inactivation (h_∞) vs membrane potential obtained by applying the protocol described in the text. To obtain values of h_∞ peak currents at −10 mV were normalized to their largest measured values. The continuous line through data points is the least-squares best fit of the Boltzmann equation $h_\infty = 1/\{1 + \exp[(V - V_{½})/k]\}$, where $V_{½}$ = −79.1 mV and k = 11.7 mV. Bars indicate SD of the means (N = 8).

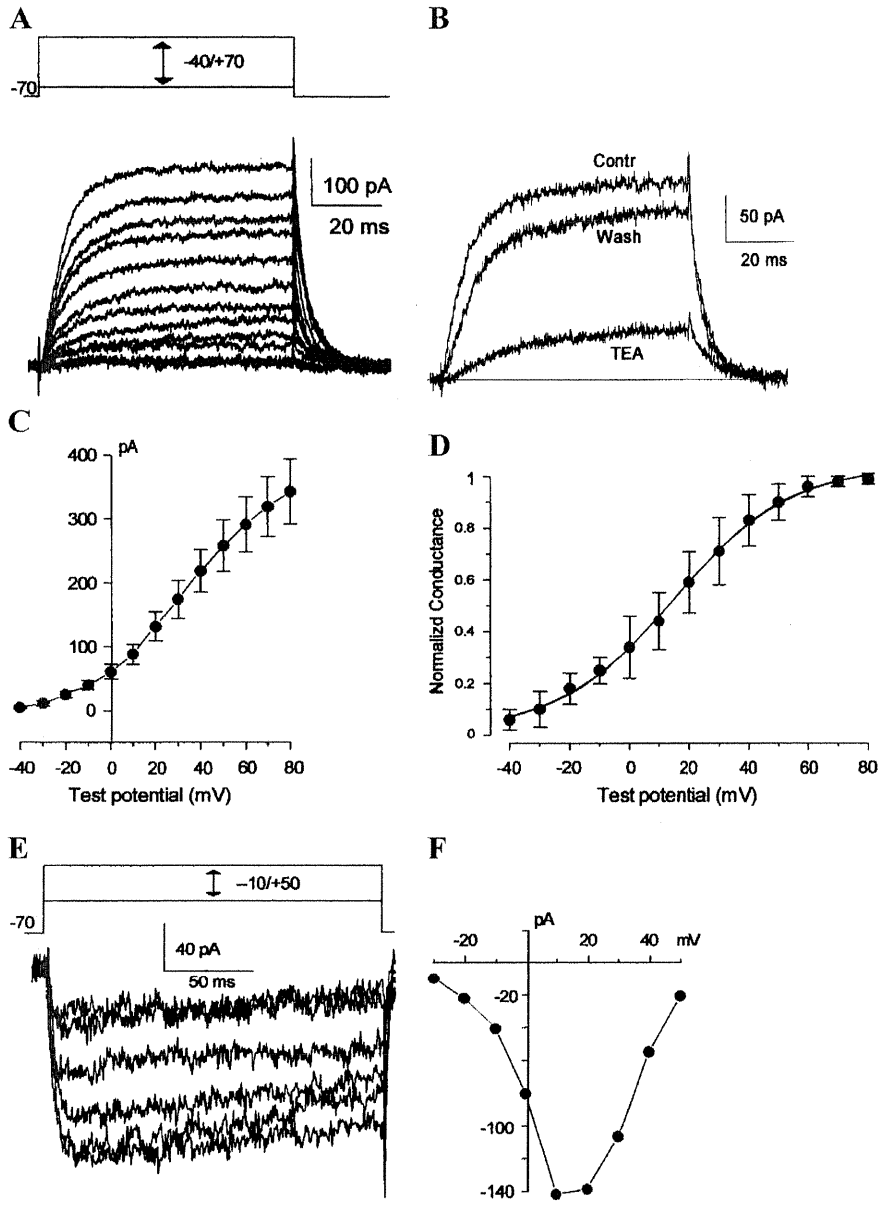

FIG. 6. Voltage-dependent potassium and calcium currents in ST14A cells. (A) Superimposed outward current traces were elicited using the voltage pulse protocol illustrated above, in the presence of extra- and intracellular saline appropriate to isolate K currents (see Experimental Procedures). (B) Effect of TEA (100 mM) on the outward current elicited in a ST14A cell. (C) Average of the outward current steady-state amplitude vs voltage (N = 7). Bars denote standard errors; holding potential −70 mV. (D) Average normalized conductance–voltage relation for the K conductance. Data are represented as means and SD (N = 7); the continuous line through data points is the least-squares best fit of the Boltzmann equation $g_{norm} = 1/\{1 + \exp[(V - V_{½})/k]\}$, where $V_{½}$ and k were 15.1 and −19.3 mV, respectively. (E) Voltage-dependent activation of slowly inactivating outward currents in a ST14A cell. Superimposed current traces were elicited in control intra- and extracellular saline appropriate to isolate Ca current (see Experimental Procedures), using the voltage pulse protocol illustrated over the current tracings. (F) Peak current–voltage relationship for a three-cell sample Ca conductance; holding potential −70 mV.

its steady-state value at any potential. The mean peak current, normalized to its maximum evoked with conditioning hyperpolarization to −130 mV, is plotted vs conditioning potential in Fig. 5F. The steady-state inactivation curve showed a sigmoidal dependence on voltage which fit the equation $h_{\infty} = 1/\{1 + \exp[(V - V_{½})/k]\}$, where $V_{½}$ = −79.1 mV and k = 11.7 mV.

Isolation and Time Course of a Voltage-Gated K Current in ST14A Cells

Under voltage-clamp conditions and using a low external Na^+ concentration and a patch pipette containing 140 mM K^+, a series of depolarizing voltage steps from −70 mV to potentials between −40 and +80 mV

elicited an outward current, as shown in Fig. 6A. This current was observed in about 40% of the clamped cells (N = 45), activated at about −30 mV, and did not display inactivation. These outward currents were suppressed by replacing K^+ with 140 mM Cs^+ in the patch pipette or significantly reduced in the presence of tetraethylammonium (TEA) in the extracellular solution (Fig. 6B). On average, TEA (100 mM) caused a current reduction of 68 ± 12% (N = 6). In contrast, focal perfusion with 5 mM 4-aminopyridine (4-AP), or lowering the holding potential from −70 to −40 mV, had little or no effect on these currents (not shown).

The peak I–V relationship for a seven-cell sample obtained over a voltage range between −40 and +80 mV and maintaining the cells at a holding potential of −70 mV is shown in Fig. 6C. The time course and voltage dependence of activation, the absence of a sizeable decrease in current amplitude at a given test potential after changing the holding potential from −70 to −40 mV, and the pharmacological evidence previously described strongly suggest that the outward current elicited in ST14A cells is classifiable as a delayed rectifier potassium current.

The activation characteristics of the K^+ current were analyzed by estimating the conductance (g) at different depolarizations according to the relation $I_K = g(V - E_K)$, where I_K refers to steady-state current values. The data were then fitted to the Boltzmann equation $g = g_{max}/\{1 + \exp[(V - V_{½})/k]\}$. The maximum conductance, g_{max}, was 2.0 ± 0.9 nS (N = 7). The average normalized conductance is shown in Fig. 6D, in which the half-activation potential, $V_{½}$, and the slope, k, were 15.1 and −19.3 mV, respectively.

Isolation and Time Course of a Ca Current in ST14A Cells

In a few ST14A cells (5/35), in the presence of 10 mM extracellular Ba^{2+} and with the patch pipette filled with 140 mM Cs^+, a series of depolarizing voltage steps from −70 mV to potentials between −30 and +50 mV elicited inward currents like those shown in Fig. 6E. In contrast to the Na currents previously described, these inward currents displayed very slow and incomplete inactivation. Furthermore they were completely blocked by 0.5 mM Ni^+ (N = 4). The peak I–V relationship for a three-cell sample is shown in Fig. 6F. It reached a peak at +10 mV and the extrapolated reversal potential was about +60 mV. According to its activation and inactivation features, ionic selectivity, and sensitivity to the Ca channel blocker Ni^+, we concluded that this outward current was a high-voltage-activated Ca channel current.

DISCUSSION

In this study, we describe the characteristics of the ST14A cell, an immortalized striatal cell line. We demonstrate that these cells express phenotypic and physiologic characteristics of neurons. In addition, we identified critically important similarities to the striatal medium-size spiny neuron.

Similar to other immortalized neuronal cell lines (29, 31), the ST14A demonstrates a flat body with few processes when in the undifferentiated state. When grown at the nonpermissive temperature or in the absence of serum, the cells developed short processes, but still lacked action potentials. The physiologic characteristics of previously described immortalized neuronal cell lines from the central nervous system have not always been examined (31, 35, 36). Fifty percent of the cells from the immortalized dorsal root ganglion cell line described by Raymon *et al.* (29) demonstrated action potentials when differentiated in medium containing forskolin and peptide growth factors. Likewise, ST14A cells, when grown in the presence of aFGF, dopamine, and agents which stimulate adenylyl cyclase and protein kinase C, developed a more neuronal appearance, with a triangular soma and a greater number of neurites of longer length. Simultaneously, βIII-tubulin, 90% of which is transported to distal axons within 2–3 days in sympathetic neurons (3), was up-regulated. Even more important, under these conditions, the cells displayed physiologic characteristics unique to neurons.

In summary, under current-clamp conditions and starting from a hyperpolarized membrane potential, intracellular injection of depolarizing current stimuli elicited overshooting action potentials in a fraction of *in vitro* differentiated ST14A cells. These regenerative voltage responses are related to the expression in these cells of functional voltage-gated channels with features corresponding to those of Na channels and delayed rectifier K channels similar to those described in neurons. Concerning the Na conductance, it displays a low sensitivity to the Na channel blocker TTX in comparison with adult neurons. Interestingly, it has been shown that in dorsal root ganglion cells as well as in skeletal muscle, neuroblastoma, and brain cells, the sensitivity of Na channels to TTX increases with the maturation of the cells (reviewed in 45). Furthermore, the potential for half-maximal inactivation of the Na conductance was between 10 and 30 mV more negative than that found in adult neurons. This value (−79 mV in average) is close to that reported for undifferentiated neuroblastoma cell lines (15, 26, 38) and for immature spinal cord neurons (25). This indicates that most of the channels are not available for activation at the resting potential in these cells. These properties are undoubtedly related to the difficulty of these cells to mount regenerative responses under current-clamp conditions when starting from their resting potential.

The outward current measured in ST14A cells has features of a "delayed rectifier" potassium conductance similar to that found in adult neurons. These include

its threshold and time course of activation, the absence of inactivation, and its pharmacological properties (blocked by external TEA and intracellular cesium ions and insensitivity to 4-AP). The maximum conductance of the K current displayed a great variability from cell to cell and its average value (2 nS) was one-third lower than that measured for the Na current (6.1 nS). These features could be related to the relatively slow action potential repolarization rate detected in most ST14A cells. On the whole, the excitability properties and those of the underlying voltage-gated channels expressed in morphologically differentiated ST14A cells are typical of neurons developing toward their adult phenotype.

The ST14A cells also display several characteristics more specific to striatal medium-size spiny neurons, albeit immature ones. All medium-size spiny striatal neurons are GABAergic, and the synthesis of GABA appears very early in development and can even be detected in the subventricular zone (23). Levels are rather low, however, until the postnatal period, when during the first 2 postnatal weeks, virtually all markers of medium-size spiny neurons rise from low to adult levels (reviewed in 11). The ST14A cell line, as determined by immunocytochemistry, is clearly GABAergic.

DARPP-32 is a dopamine- and cyclic AMP-regulated phosphoprotein which is expressed in 98% of the medium-size spiny neurons (27). Developmentally, DARPP-32 is first detected at E14 in the rat, in scattered cells in the mantle layer of the developing striatum, and along the lateral edge (12). DARPP-32 is undetectable in the ventricular or subventricular zone, implying that DARPP-32 gene expression does not begin until the neurons are postmitotic and postmigrational. ARPP-21 is immunocytochemically undetectable in mouse striatum until E18 (21). As shown, not all similarly immortalized cell lines express DARPP-32. What is unknown is whether the characteristics of isolated clones represent the expression of genes already present at the time of retroviral transduction or whether genes are newly transcribed as these cells divide, prior to their cloning. Thus, the ST14A cell may represent a medium-size spiny neuron which was already expressing DARPP-32 at the time of immortalization or an immortalized progenitor cell already programmed to ultimately become a medium-size spiny neuron. We favor the latter explanation, since the ST14A cells also express nestin, which is not expressed in postmitotic cells. Either way, the coexpression of DARPP-32 and nestin appears to be an artifact of the immortalization procedure. It will be interesting to determine whether conditions which induce the expression of DARPP-32 in the ST86 and ST79-13a lines can be identified. Future experiments will also determine whether with prolonged maturation, either in the dopamine differentiation mix or with the addition of growth factors known to induce MSN maturation *in vivo* and *in vitro* (21), the ST14A line can be induced to express ARPP-21 and to express electrophysiological characteristics of more mature neurons. In this regard, it is important to note that over one-quarter of medium-size spiny neurons express DARPP-32 when grown in Neurobasal B27 medium in the absence of neurotrophins, but that expression of ARPP-21 requires neurotrophins (21).

DARPP-32 is an integral part of the dopaminoceptive signal transduction pathway, a key feature of medium-size spiny neurons (18). Both D1- and D2-receptor subtypes are expressed early in development in the striatum (33). Despite the enrichment of both D1 receptors and DARPP-32 in striatal patch neurons on P0 (16), D1-stimulated adenylyl cyclase activity at birth is barely above baseline cyclase activity (33). In the ST14A cell line, D1-subtype receptors appear to represent a minority of the functional dopamine receptors. Therefore, it is not surprising that in these MSN-like cells, measurable stimulation of adenylyl cyclase activity by dopamine is not convincingly present. The robust stimulation of phosphorylation of CREB following treatment of the cells with dopamine is explained by the presence of functional D2-like receptors, as determined by the antagonism of this effect with eticlopride. Unlike the D1 receptor, D2-subtype receptors do not utilize the adenylyl cyclase pathway to stimulate phosphorylation of CREB. Rather, in striatal brain slices, this effect appears to be mediated via protein kinase C, Ca^{2+}/calmodulin-dependent protein kinase, and DARPP-32 (44). Future studies will identify the actual pathway utilized in ST14A cells.

These combined data place the ST14A cell line in a selected group of cell lines which resemble neuronal subtypes from which they were derived. The utility of this cell line is enhanced by the ease with which the cells are both stably and transiently transfected, resulting in high levels of expression of exogenous genes (5, 32). The specific resemblance of the ST14A cell line to a medium-size spiny neuron has already been exploited to model striatal pathology by the expression of mutant huntingtin (32). The use of the ST14A cell line for *in vivo* studies of brain development, damage, and repair is further enhanced by its extended survival and restricted growth (24). As with other similarly derived cell lines, ST14A cells have been successfully transplanted into adult (9, 24) and developing (4) rodent brains for studies on cell differentiation and regulated delivery of exogenous genes (9), including antitumoral agents (2).

ACKNOWLEDGMENTS

This work was supported by the Hereditary Disease Foundation (U.S.A.), the Huntington's Disease Society of America (U.S.A.) and, partially, by Telethon (Italy, E840) to E.C., Telethon (Italy, E1025) to L.C., and The Research Foundation for Mental Hygiene to

M.E.E. E.C. and M.E.E. were also supported by a NATO Collaborative Research Grant (960204).

REFERENCES

1. Almazan, G., and R. D. G. McKay. 1992. An oligodendrocyte precursor cell line from optic nerve. *Brain Res.* 579: 234–245.
2. Benedetti, S., B. Pirola, B. Pollo, L. Magrassi, M. G. Bruzzone, D. Rigamonti, R. Galli, C. DeFraja, F. Di Meco, Vescovi A., E. Cattaneo, and G. Finocchiaro. 2000. Gene therapy of experimental brain tumors using neural progenitor cells. *Nature Med.* 6: 447–450.
3. Campenot, R. B., K. Lund, and D. L. Senger. 1996. Delivery of newly synthesized tubulin to rapidly growing distal axons of sympathetic neurons in compartmented cultures. *J. Cell Biol.* 135: 701–709.
4. Cattaneo, E., L. Magrassi, G. Butti, L. Santi, A. Giavazzi, and S. Pezzotta. 1994. A short term analysis of the behaviour of conditionally immortalized neuronal progenitors and primary neuroepithelial cells implanted into the fetal rat brain. *Dev. Brain Res.* 83: 197–208.
5. Cattaneo, E., C. De-Fraja, L. Conti, B. Reinach, L. Bolis, S. Govoni, and E. Liboi. 1996. Activation of the Jak/STAT pathway leads to proliferation of ST14A central nervous system progenitor cells. *J. Biol. Chem.* 271: 23374–23379.
6. Cattaneo, E., and L. Conti. 1998. Generation and characterization of embryonic striatal conditionally immortalized ST14A cells. *J. Neurosci. Res.* 53: 223–234.
7. Cole, D. G., L. A. Kobierski, C. Konradi, and S. E. Hyman. 1994. 6-Hydroxydopamine lesions of rat substantia nigra up-regulate dopamine-induced phosphorylation of the cAMP-response element-binding protein in striatal neurons. *Proc. Natl. Acad. Sci. USA* 91: 9631–9635.
8. Conti, L., C. De Fraja, M. Gulisano, E. Migliaccio, S. Govoni, and E. Cattaneo. 1997. Expression and activation of SH2/PTB-containing ShcA adaptor protein reflects the pattern of neurogenesis in the mammalian brain. *Proc. Natl. Acad. Sci. USA* 94: 8185–8190.
9. Corti, O., P. Horellou, P. Colin, E. Cattaneo, and J. Mallet. 1996. Intracerebral tetracycline-dependent regulation of gene expression in grafts of neural precursors. *NeuroReport* 7: 1655–1659.
10. Du, X., N. D. Stull, and L. Iacovitti. 1994. Novel expression of the tyrosine hydroxylase gene requires both acidic fibroblast growth factor and an activator. *J. Neurosci.* 14: 7688–7694.
11. Ehrlich, M. E., N. L. Rosen, T. Kurihara, I. A. Shalaby, and P. Greengard. 1990. DARPP-32 development in the caudate nucleus is independent of afferent input from the substantia nigra. *Dev. Brain Res.* 54: 257–263.
12. Foster, G. A., M. Schultzberg, T. Hokfelt, M. Goldstein, H. C. Hemmings, Jr., C. C. Ouimet, S. I. Walaas, and P. Greengard. 1988. Ontogeny of the dopamine and cyclic adenosine-3′:5′-monophosphate-regulated phosphoprotein (DARPP-32) in the pre- and postnatal mouse central nervous system. *Int. J. Dev. Neurosci.* 6: 367–386.
13. Frederiksen, K., P. S. Jat, N. Valtz, D. Levy, and R. D. G. McKay. 1988. Immortalization of precursor cells from the mammalian CNS. *Neuron* 1: 439–448.
14. Giordano, M., H. Takashima, A. Herranz, M. Poltorak, H. M. Geller, M. Marone, and W. J. Freed. 1993. Immortalized GABAergic cell lines derived from rat striatum using temperature-sensitive allele of the SV40 large T antigen. *Exp. Neurol.* 124: 395–400.
15. Godoy, C. M. G., and S. Cukierman. 1994. Multiple effects of protein kinase C activators on Na^+ currents in mouse neuroblastoma cells. *J. Membr. Biol.* 140: 101–110.
16. Graybiel, A. M. 1990. Neurotransmitters and neuromodulators in the basal ganglia. *Trends Neurosci.* 13: 244–254.
17. Greene, L. A., and A. S. Tischler. 1976. Establishment of a noradrenergic clonal cell line of rat pheochromocytoma cells which respond to nerve growth factor. *Proc. Natl. Acad. Sci. USA* 73: 2424–2428.
18. Greengard, P., P. B. Allen, and A. C. Nairn. 1999. Beyond the dopamine receptor: The DARPP-32/protein phosphatase-1 cascade. *Neuron* 23: 435–447.
19. Hamill, O. P., A. Marty, E. Neher, B. Sakmann, and Sigworth. 1981. Improved patch clamp techniques for high-resolution current recording from cells and cell-free membrane patches. *Pflugers Arch.* 391: 85–100.
20. Ivkovic, S., O. Polonskaia, I. Farinas, and M. E. Ehrlich. 1997. Brain-derived neurotrophic factor regulates maturation of the DARPP-32 phenotype in striatal medium size spiny neurons: Studies in vivo and in vitro. *Neuroscience* 79: 509–516.
21. Ivkovic, S., and M. E. Ehrlich. 1999. Expression of the striatal DARPP-32/ARPP-21 phenotype in GABAergic neurons requires neurotrophins in vivo and in vitro. *J. Neurosci.* 19: 5409–5419.
22. Jat, P. S., and P. A. Sharp. 1989. Cell line established by a temperature-sensitive simian virus 40 large-T-antigen gene are growth restricted at the nonpermessive temperature. *Mol. Cell. Biol.* 9: 1672–1681.
23. Lauder, J. M., V. K. M. Han, P. Henderson, T. Verdooorn, and A. C. Towle. 1986. Prenatal ontogeny of the GABAergic system in the rat brain: An immunocytochemical study. *Neuroscience* 19: 465–493.
24. Lundberg, C., A. Martinez-Serrano, E. Cattaneo, D. G. McKay, and A. Bjorklund. 1997. Survival, integration and differentiation of neural stem cell lines after transplantation to the adult rat striatum. *Exp. Neurol.* 145: 342–360.
25. MacDermott, A. B., and G. L. Westbrook. 1986. Early development of voltage-dependent sodium currents in cultured mouse spinal cord neurons. *Dev. Biol.* 113: 317–326.
26. Moran, O., and F. Conti. 1990. Sodium ionic and gating currents in mammalian cells. *Eur. Biophys. J.* 18: 25–32.
27. Ouimet, C. C., H. C. Hemmings, Jr., and P. Greengard. 1989. ARPP-21, a cyclic AMP-regulated phosphoprotein enriched in dopamine-innervated brain regions. II. Immunocytochemical localization in rat brain. *J. Neurosci.* 9: 865–875.
28. Ouimet, C. C., K. C. Langley-Guillion, and P. Greengard. 1998. Quantitative immunocytochemistry of DARPP-32-expressing neurons in the rat caudatoputamen. *Brain Res.* 808: 8–12.
29. Raymon, H. K., S. Thode, J. Zhou, G. C. Friedman, J. R. Pardinas, C. Barrere, R. M. Johnson, and D. W. Y. Sah. 1999. Immortalized human dorsal root ganglion cells differentiate into neurons with nociceptive properties. *J. Neurosci.* 19: 5420–5428.
30. Redies, C., U. Lendahl, and R. D. G. McKay. 1991. Differentiation and heterogeneity in T-antigen immortalized precursor cell lines from mouse cerebellum. *J. Neurosci. Res.* 30: 601–615.
31. Renfranz, P. J., M. G. Cunningham, and R. D. G. McKay. 1991. Region-specific differentiation of the hippocampal stem cell line HiB5 upon implantation into the developing mammalian brain. *Cell* 66: 713–729.
32. Rigamonti, D., J. H. Bauer, C. De-Fraja, L. Conti, S. Sipione, C. Sciorati, E. Clementi, A. Hackam, M. Hyden, Y. Li, C. Ross, S. Govoni, C. Vincenz, and E. Cattaneo. 2000. Wild-type huntingtin protects from apoptosis upstream of caspase-3. *J. Neurosci.* 20: 3705–3713.

33. Rius, R. A., S. Mollner, T. Pfeuffer, Y. P. Loh. 1994. Developmental changes in Gs and Golf proteins and adenylyl cyclases in mouse brain membranes. *Brain Res.* 643: 50–58.

34. Ryder, E. F., E. Y. Snyder, and C. L. Cepko. 1990. Establishment and characterization of multipotent neural cell lines using retrovirus vector-mediated oncogene transfer. *J. Neurobiol.* 21: 356–375.

35. Snyder, E. Y., D. L. Deichter, C. Walsh, S. Arnold-Aldea, E. A. Hartwieg, and C. L. Cepko. 1992. Multipotent neural cell lines can engraft and participate in development of mouse cerebellum. *Cell* 68: 33–51.

36. Son, J. H., H. S. Chun, T. H. Joh, S. Cho, B. Conti, and J. W. Lee. 1999. Neuroprotection and neuronal differentiation studies using substantia nigra dopaminergic cells derived from transgenic mouse embryos. *J. Neurosci.* 19: 10–20.

37. Surmeir, D. J., W. J. Song, and Z. Yan. 1996. Coordinated expression of dopamine receptors in neostriatal medium size spiny neurons. *J. Neurosci.* 16: 6579–6591.

38. Toselli, M., P. Tosetti, and V. Taglietti. 1996. Functional changes in sodium conductance in the human neuroblastoma cell line SH-SY5Y during in vitro differentiation. *J. Neurophysiol.* 76: 3920–3927.

39. Unterwald, E. M., B. M. Cox, M. J. Kreek, T. E. Cote, and S. Izenwasser. 1993. Chronic repeated cocaine administration alters basal and opioid-regulated adenylyl cyclase activity. *Synapse* 15: 33–38.

40. Wainwright, M. S., B. D. Perry, L. A. Won, K. L. O'Malley, E.-Y. Wang, M. E. Ehrlich, and A. Heller. 1995. Immortalized murine striatal neuronal cell lines expressing dopamine receptors and cholinergic properties. *J. Neurosci.* 15: 676–688.

41. White, L. A., and S. R. Whittemore. 1992. Immortalization of raphe neurons: An approach to neuronal function in vitro and in vivo. *J. Chem. Neuroanat.* 5: 327–330.

42. Whittemore, S. R., and L. A. White. 1993. Target regulation of neuronal differentiation in a temperature-sensitive cell line derived from medullary raphe. *Brain Res.* 615: 27–40.

43. Whittemore, S. R., J. T. Neary, N. Kleitman, H. R. Sanon, A. Benigno, R. P. Donahue, and M. D. Norenberg. 1994. Isolation and characterization of conditionally immortalized astrocyte cell lines derived from adult human spinal cord. *GLIA* 10: 211–226.

44. Yan, Z., J. Feng, A. A. Fienberg, and P. Greengard. 1999. D-2 dopamine receptors induce mitogen-activated protein kinase and cAMP response element-binding protein phosphorylation in neurons. *Proc. Natl. Acad. Sci. USA* 96: 11607–11612.

45. Yoshida, S. 1994. Tetrodotoxin-resistant sodium channels. *Cell. Mol. Neurobiol.* 14: 227–244.